Automatica 144 (2022) 110486

Contents lists available at ScienceDirect

Automatica

journal homepage: www.elsevier.com/locate/automatica

Identification of linear systems with multiplicative noise from multiple trajectory data ☆

Yu Xing [a,*,1], Benjamin Gravell [b,1], Xingkang He [c], Karl Henrik Johansson [a], Tyler H. Summers [b]

[a] Division of Decision and Control Systems, School of Electrical Engineering and Computer Science, KTH Royal Institute of Technology, and Digital Futures, Stockholm, Sweden
[b] Department of Mechanical Engineering, The University of Texas at Dallas, Richardson, TX, USA
[c] Department of Electrical Engineering, University of Notre Dame, South Bend, IN, USA

ARTICLE INFO

Article history:
Received 2 July 2021
Received in revised form 12 January 2022
Accepted 13 May 2022
Available online 12 July 2022

Keywords:
Linear system identification
Multiplicative noise
Multiple trajectories
Non-asymptotic analysis

ABSTRACT

The paper studies identification of linear systems with multiplicative noise from multiple-trajectory data. An algorithm based on the least-squares method and multiple-trajectory data is proposed for joint estimation of the nominal system matrices and the covariance matrix of the multiplicative noise. The algorithm does not need prior knowledge of the noise or stability of the system, but requires only independent inputs with pre-designed first and second moments and relatively small trajectory length. The study of identifiability of the noise covariance matrix shows that there exists an equivalent class of matrices that generate the same second-moment dynamic of system states. It is demonstrated how to obtain the equivalent class based on estimates of the noise covariance. Asymptotic consistency of the algorithm is verified under sufficiently exciting inputs and system controllability conditions. Non-asymptotic performance of the algorithm is also analyzed under the assumption that the system is bounded. The analysis provides high-probability bounds vanishing as the number of trajectories grows to infinity. The results are illustrated by numerical simulations.

1. Introduction

The study of stochastic systems with multiplicative noise (i.e., system states and inputs multiplied by noise) has a long history in control theory (Wonham, 1967), and is re-emerging in the context of complex networked systems and learning-based control. In contrast to the additive-noise setting, the multiplicative-noise modeling framework has the ability to capture coupling between noise and system states. This situation occurs in modern control systems as diverse as robotics with distance-dependent sensor errors (Du Toit & Burdick, 2011), networked systems with noisy communication channels (Antsaklis & Baillieul, 2007; Hespanha et al., 2007), modern power networks with high penetration of intermittent renewables (Guo & Summers, 2019), turbulent fluid flow (Lumley, 2007), and neuronal brain networks (Breakspear, 2017). Linear systems with multiplicative noise are particularly attractive as a stochastic modeling framework because they remain simple enough to admit closed-form expressions for stabilization (Boyd et al., 1994) and optimal control (Gravell et al., 2021; Kleinman, 1969; Wonham, 1967).

It is important to study identification of linear systems with multiplicative noise, because, when solving problems such as control design of multiplicative-noise linear quadratic regulator (LQR), system parameters including the nominal system matrices and the noise covariance matrix, especially the latter, generally need be known (Gravell et al., 2021). In contrast, for the design problem of additive-noise LQR, the covariance matrix of additive noise needs not be known (Dean et al., 2019). Moreover, the identification problem requires further investigation; for instance, it is unclear how to formally quantify identifiability issues resulting from coupling between system states and multiplicative noise, and how to design identification algorithms to efficiently tackle the influence of multiplicative noise.

Another issue that must be addressed is how to perform system identification based on multiple-trajectory data, rather than on single-trajectory data. Multiple-trajectory data arises in

☆ This work was supported by the Air Force Office of Scientific Research, USA under award number FA2386-19-1-4073, the National Science Foundation, USA under award number ECCS-2047040, the Knut & Alice Wallenberg Foundation, Sweden, and the Swedish Research Council. The 2020 American Control Conference, July 1–3, 2020, Denver, CO, USA. This paper was recommended for publication in revised form by Associate Editor Ali Zemouche under the direction of Editor Alessandro Chiuso.

* Corresponding author.
E-mail addresses: yuxing2@kth.se (Y. Xing), Benjamin.Gravell@utdallas.edu (B. Gravell), xhe9@nd.edu (X. He), kallej@kth.se (K.H. Johansson), Tyler.Summers@utdallas.edu (T.H. Summers).

[1] Y. Xing and B. Gravell contributed equally to this paper.

https://doi.org/10.1016/j.automatica.2022.110486

two broad situations: (1) episodic tasks where a system is reset to an initial state after a finite run time, as encountered in iterative learning control and reinforcement learning (Matni et al., 2019); and (2) data collected from multiple identical systems in parallel, for example, robotic-grasping dataset collected by Google running several robot arms concurrently (Gu et al., 2017; Levine et al., 2018). For multiple-trajectory data, the length of each trajectory may be small, but the number of trajectories can be large. However, the classic literature of system identification mainly focuses on studying online estimation over a single trajectory, so there is a need to study how to identify systems based on multiple-trajectory data. In addition, system identification based on multiple trajectories can be a pre-step of conducting other tasks such as control design of LQR (Dean et al., 2019). Thus, studying the performance of identification algorithms based on multiple trajectories is necessary for obtaining performance guarantees of later tasks.

1.1. Related work

For identification of a nominal linear system, recursive algorithms, such as the recursive least-squares algorithm, have been developed in the control literature (Chen & Guo, 2012; Lai & Wei, 1982; Ljung, 1986). These algorithms can be applied to identification of linear systems with multiplicative noise, provided that certain conditions of system stability and noise hold. Non-asymptotic performance analysis of identification methods can be found in Campi and Weyer (2002, 2005) and Weyer and Campi (2002). It has once again attracted attention from different domains and been investigated more extensively, because of recent development of random matrix theories, self-normalized martingales, and so on (see Dean et al. (2019), Matni and Tu (2019) and Zheng and Li (2020) and references therein).

For estimation of noise covariance, both recursive and batch methods have been proposed over the last few decades (Duník et al., 2017), but most of these methods focus on the additive-noise case. In order to estimate multiplicative noise covariance, Schön et al. (2011) introduces a maximum-likelihood approach, and Kantas et al. (2015), Kitagawa (1998) utilize Bayesian frameworks. These methods, however, require prior assumptions on the noise distributions, whose incorrectness may worsen algorithm performance. Coppens and Patrinos (2020) and Coppens et al. (2020) study stochastic LQR design for a special case of linear systems with multiplicative noise. It is assumed that the multiplicative noise is observed directly such that a concentration inequality can be obtained for estimates of the noise covariance. The most relevant work to our paper is Di and Lamperski (2021), which studies simultaneously estimating the nominal system parameters and noise covariance matrix based on single-trajectory data. In that paper, a self-normalizing (ellipsoidal) bound and a Euclidean (box) bound are provided for least-squares estimates, but it is not clear whether the bounds converge to zero under the setting of linear systems with multiplicative noise.

There is a growing interest in system identification based on multiple-trajectory data, along with their applications in data-driven control (Dean et al., 2019; Matni & Tu, 2019), due to the powerful and convenient estimator schemes facilitated by resetting the system. This framework can be applied to both stable and unstable systems, because of the finite duration of each trajectory. The authors in Tu and Recht (2018) and Sun et al. (2020) introduce the procedure of collecting multiple trajectories, to identify finite impulse response systems. In Dean et al. (2019), the authors develop a framework called coarse-ID control to solve the problem of LQR with unknown linear dynamics. The first step of this framework is to learn a coarse model of the unknown linear system, by observing multiple independent trajectories with finite length. However, only the last input-state pairs of the trajectories are used in the theoretical analysis of the learning algorithm. The performance of a least-squares algorithm, using all samples of every trajectory, is studied in Zheng and Li (2020), for partially observed, possibly open-loop unstable, linear systems.

1.2. Contributions

This paper considers identification of linear systems with multiplicative noise from multiple-trajectory data. The contributions are three-fold:

1. An algorithm (Algorithm 1) based on the least-squares method and multiple-trajectory data is proposed for joint identification of the nominal system matrices and the multiplicative noise covariance from multiple-trajectory data. The algorithm does not need prior knowledge of the noise or stability of the system, but requires only independent inputs with pre-designed first and second moments, relatively small length for each trajectory, and the assumption of independent and identically distributed (i.i.d.) noise with finite first and second moments. It is theoretically shown that, under the preceding conditions, the algorithm solves the identification problem.
2. Identifiability of the noise covariance matrix is investigated (Propositions 1 and 2). It is shown that there exists an equivalent class of covariance matrices that generate the same second-moment dynamic of system states. In addition, it is studied when such equivalent class has a unique element, meaning that the covariance matrix can be uniquely determined. An explicit expression of the equivalent class is provided for the recovery of the noise covariance based on estimates given by the proposed algorithm.
3. Asymptotic consistency of the proposed algorithm is verified (Theorem 1), under sufficiently exciting inputs and system controllability conditions. Non-asymptotic estimation performance is also analyzed under the assumption that the system is bounded. This analysis provides high-probability error bounds, which vanish as the number of trajectories grows to infinity (Theorems 2 and 3).

Compared with Di and Lamperski (2021), the current paper provides high-probability error bounds, for the proposed algorithm, that converge to zero as the number of trajectories increases. In addition, identifiability of the noise covariance matrix is thoroughly studied, and conditions, under which the covariance matrix is uniquely determined, are provided. In our problem, because of the complicated structure of the second-moment dynamic of system states, both analysis of the error bounds and study of the identifiability require more elaborate use of tools from linear algebra and high-dimensional probability theory. The differences between this paper and its conference version (Xing et al., 2020) are as follows. This paper studies identifiability of the noise covariance matrix in detail, demonstrating a framework to recover the equivalent class of covariance matrices. Moreover, sharper bounds for the required length of each trajectory are obtained. Finally, finite sample analysis of the proposed algorithm is provided.

1.3. Outline

The remainder of the paper is organized as follows. The problem is formulated in Section 2. In Section 3 the algorithm is introduced and theoretical results are given. Numerical simulation results are presented in Section 4. Section 5 concludes

the paper. Due to page limit, proofs are put into the extended version (Xing et al., 2021).

Notation. Denote the n-dimensional Euclidean space by $\mathbb{R}^n$, and the set of $n \times m$ real matrices by $\mathbb{R}^{n\times m}$. Let $\mathbb{N}$ stand for the set of nonnegative integers, and $\mathbb{N}^+ := \mathbb{N} \setminus \{0\}$. Let $[k] := \{1, 2, \ldots, k\}$, $k \in \mathbb{N}^+$. Denote the Euclidean norm of vectors by $\|\cdot\|$, and the spectral norm of matrices by $\|\cdot\|_2$. The probability of an event E is denoted by $\mathbb{P}\{E\}$, and the expectation of a random vector x is represented by $\mathbb{E}\{x\}$. An event happening almost surely (a.s.) means that it happens with probability one. Let $A \times B$ be the Cartesian product of sets A and B, namely, $A \times B = \{(a, b) : a \in A, b \in B\}$. For two sequences of real numbers a_k and $b_k \neq 0$, $k \in \mathbb{N}^+$, denote $a_k = \mathcal{O}(b_k)$, if there exists a positive constant C such that $|a_k/b_k| \leq C$ for all $k \in \mathbb{N}^+$. Let a_{ij} or $[A]_{ij}$ represent the (i, j)th entry of $A \in \mathbb{R}^{n\times m}$. Denote the n-dimensional all-one vector and all-zero vector by $\mathbf{1}_n$ and $\mathbf{0}_n$, respectively. The n-dimensional unit vector with ith component being one is represented by $\mathbf{e}_i^n$. I_n is the n-dimensional identity matrix. For two symmetric matrices $A, B \in \mathbb{R}^{n\times n}$, $A \succeq 0$ ($A \succ 0$) means that A is positive semidefinite (positive definite), and $A \succeq B$ ($A \succ B$) means that $A - B \succeq 0$ ($A - B \succ 0$). A block diagonal matrix A with $A_1, \ldots, A_k$ on its diagonal is denoted by $\mathrm{blockdiag}(A_1, \ldots, A_k)$. The Kronecker product of two matrices $A \in \mathbb{R}^{m\times n}$ and $B \in RR^{p\times q}$ is represented by $A\otimes B$. The full vectorization of $A = [a_{ij}] \in \mathbb{R}^{m\times n}$ is found by stacking the columns of A (i.e., $\mathrm{vec}(A) = [a_{11}\ a_{21}\ \cdots\ a_{m1}\ a_{12}\ a_{22}\ \cdots\ a_{mn}]^\intercal$). The symmetric vectorization (also called half-vectorization) of a symmetric matrix $A \in \mathbb{R}^{n\times n}$ is found by stacking the upper triangular part of the columns of A (i.e., $\mathrm{svec}(A) = [a_{11}\ a_{12}\ a_{22}\ \cdots\ a_{1n}\ a_{2n}\ \cdots\ a_{nn}]^\intercal$). The inverse operations of $\mathrm{vec}(\cdot)$ and $\mathrm{svec}(\cdot)$, given $p, q \in \mathbb{N}$, are the full matricization $\mathrm{mat}_{p\times q}(x) := (\mathrm{vec}(I_q)^\intercal \otimes I_p)(I_q \otimes x)$ for a vector $x \in \mathbb{R}^{pq}$ and symmetric matricization $\mathrm{smat}_p(y)$ for a vector $y \in \mathbb{R}^{p(p+1)/2}$, respectively. To generalize the vectorization and matricization operations to a block matrix

$$B = \begin{bmatrix} B_{11} & B_{12} & \cdots & B_{1n} \\ \vdots & \vdots & & \vdots \\ B_{m1} & B_{m2} & \cdots & B_{mn} \end{bmatrix} \in \mathbb{R}^{mp\times nq},$$

where $B_{ij} \in \mathbb{R}^{p\times q}$, define the following matrix reshaping operator $F : \mathbb{R}^{mp\times nq} \to \mathbb{R}^{mn\times pq}$,

$$F(B, m, n, p, q) := [\mathrm{vec}(B_{11})\ \mathrm{vec}(B_{21})\ \cdots\ \mathrm{vec}(B_{m1})\ \mathrm{vec}(B_{12})\ \mathrm{vec}(B_{22})\ \cdots\ \mathrm{vec}(B_{mn})]^\intercal.$$

Then it holds that $F(A \otimes A, m, n, m, n) = \mathrm{vec}(A)\,\mathrm{vec}(A)^\intercal$ for $A \in \mathbb{R}^{m\times n}$, which demonstrates the correspondence between the entries of $A \otimes A$ and those of $\mathrm{vec}(A)\,\mathrm{vec}(A)^\intercal$. Note that, when $p = q = 1$, $F(\cdot)$ degenerates to $\mathrm{vec}(\cdot)$. Define the inverse reshaping operator $G : \mathbb{R}^{mn\times pq} \to \mathbb{R}^{mp\times nq}$ as

$$G(B, m, n, p, q) := \begin{bmatrix} \mathrm{mat}_{p\times q}(B_1) & \cdots & \mathrm{mat}_{p\times q}(B_{(n-1)m+1}) \\ \mathrm{mat}_{p\times q}(B_2) & \cdots & \mathrm{mat}_{p\times q}(B_{(n-1)m+2}) \\ \vdots & & \vdots \\ \mathrm{mat}_{p\times q}(B_m) & \cdots & \mathrm{mat}_{p\times q}(B_{mn}) \end{bmatrix},$$

where $B \in \mathbb{R}^{mn\times pq}$, $B_i^\intercal$ is the ith row of B. Thus F and G are inverses of each other in the sense that

$$F(G(A, m, n, p, q), m, n, p, q) = A,$$
$$G(F(B, m, n, p, q), m, n, p, q) = B,$$

for any $A \in \mathbb{R}^{mn\times pq}$ and $B \in \mathbb{R}^{mp\times nq}$. In this way, $G(\mathrm{vec}(A)\,\mathrm{vec}(A)^\intercal, m, n, m, n) = A\otimes A$ for $A \in \mathbb{R}^{m\times n}$. Note that both F and G are linear: $F(A + B, m, n, p, q) = F(A, m, n, p, q) + F(B, m, n, p, q)$ for $A, B \in \mathbb{R}^{mp\times nq}$, and $G(A + B, m, n, p, q) = G(A, m, n, p, q) + G(B, m, n, p, q)$ for $A, B \in \mathbb{R}^{mn\times pq}$.

2. Problem formulation

Consider the linear system with multiplicative noise

$$x_{t+1} = (A + \bar{A}_t)x_t + (B + \bar{B}_t)u_t,\ t \in \mathbb{N}, \tag{1}$$

where $x_t \in \mathbb{R}^n$ is the system state, and $u_t \in \mathbb{R}^m$ is the control input, $m \leq n$. The system is described by the nominal dynamic matrix $A \in \mathbb{R}^{n\times n}$ and the nominal input matrix $B \in \mathbb{R}^{n\times m}$, and incorporates multiplicative noise terms modeled by i.i.d. and mutually independent random matrices $\bar{A}_t$ and $\bar{B}_t$, which have zero mean and covariance matrices $\Sigma_A := \mathbb{E}\{\mathrm{vec}(\bar{A}_t)\,\mathrm{vec}(\bar{A}_t)^T\} \in \mathbb{R}^{n^2\times n^2}$ and $\Sigma_B := \mathbb{E}\{\mathrm{vec}(\bar{B}_t)\,\mathrm{vec}(\bar{B}_t)^T\} \in \mathbb{R}^{nm\times nm}$, respectively. The multiplicative noise is assumed to be independent of the inputs. Note that if $\bar{A}_t$ and $\bar{B}_t$ have non-zero means $\bar{A}$ and $\bar{B}$, respectively, then we can consider a system with nominal matrix $[A+\bar{A}\ B+\bar{B}]$, as well as noise terms $\bar{A}_t - \bar{A}$ and $\bar{B}_t - \bar{B}$, which satisfies the preceding zero-mean assumption. The term multiplicative noise refers to that noise, $\bar{A}_t$ and $\bar{B}_t$, enters the system as multipliers of x_t and u_t, rather than as additions. The independence of $\bar{A}_t$ and $\bar{B}_t$ is assumed for simplicity, and under this assumption the covariance matrix of the entire multiplicative noise is a block diagonal matrix $\mathbb{E}\{\mathrm{vec}([\bar{A}_t\ \bar{B}_t])\,\mathrm{vec}([\bar{A}_t\ \bar{B}_t])^\intercal\} = \mathrm{blockdiag}(\Sigma_A, \Sigma_B)$. Throughout the paper, we use $(\Sigma_A, \Sigma_B) \in \mathbb{R}^{n^2\times n^2} \times \mathbb{R}^{nm\times nm}$ to represent this matrix. If $\bar{A}_t$ and $\bar{B}_t$ are dependent, there is an extra but amenable term on their correlations, $\mathbb{E}\{\mathrm{vec}(\bar{A}_t)\,\mathrm{vec}(\bar{B}_t)^\intercal\}$.

An example of System (1) is the following system studied in the optimal control literature (Boyd et al., 1994; Gravell et al., 2021),

$$x_{t+1} = \Big(A + \sum_{i=1}^{r} A_i p_{i,t}\Big)x_t + \Big(B + \sum_{j=1}^{s} B_j q_{j,t}\Big)u_t, \tag{2}$$

where $\{p_{i,t}\}$ and $\{q_{i,t}\}$ are mutually independent scalar random variables, with $\mathbb{E}\{p_{i,t}\} = \mathbb{E}\{q_{j,t}\} = 0$, $\mathbb{E}\{p_{i,t}^2\} = \sigma_i^2$, and $\mathbb{E}\{q_{j,t}^2\} = \delta_j^2$, $\forall i \in [r], j \in [s], t \in \mathbb{N}$. It can be seen that $\bar{A}_t = \sum_{i=1}^r A_i p_{i,t}$ and $\bar{B}_t = \sum_{j=1}^s B_j q_{j,t}$, where σ_i and δ_j are the eigenvalues of Σ_A and Σ_B, and A_i and B_j are the reshaped eigenvectors of Σ_A and Σ_B. These parameters are necessary for optimal controller design (Gravell et al., 2021). It is also possible to use System (2) to model cyber–physical systems in which fault signals appear as multiplicative noise (Wang et al., 2020). For new systems with unknown parameters, the key problem is to identify the parameters in the first place. Another example of System (1) is interconnected systems, where the nominal part captures relationships between different subsystems, and multiplicative noise characterizes randomly varying topologies (Haber & Verhaegen, 2014).

In the rest of the paper, a trajectory sample is referred to as a *rollout*. Suppose that multiple rollouts consisting of system states and inputs (i.e., $\{[x_0^{(k)}, u_0^{(k)}, \ldots, x_{\ell-1}^{(k)}, u_{\ell-1}^{(k)}, x_\ell^{(k)}], k \in [n_r]\}$) are available, where $[x_0^{(k)}, u_0^{(k)}, \ldots, x_{\ell-1}^{(k)}, u_{\ell-1}^{(k)}, x_\ell^{(k)}]$ is the kth trajectory, ℓ is the length (index of the final time-step) of every rollout, and n_r is the number of rollouts. The problem considered in this paper is as follows.

Problem. Given multiple-trajectory data $\{[x_0^{(k)}, u_0^{(k)}, \ldots, x_{\ell-1}^{(k)}, u_{\ell-1}^{(k)}, x_\ell^{(k)}], k \in [n_r]\}$, estimate the nominal system matrix $[A\ B]$ and the noise covariance matrix (Σ_A, Σ_B).

3. Identification algorithm based on least-squares and multiple-trajectory data

In this section, we propose and study an identification algorithm solving the considered problem. Section 3.1 studies identifiability of the noise covariance matrix, paving the way to

algorithm design. Consistency of the algorithm is given by Theorem 1 in Section 3.2. Finally, sample complexity of the algorithm is studied in Section 3.3, and the results are provided in Theorems 2 and 3.

3.1. Moment dynamics and algorithm design

In this subsection, we propose an algorithm based on multiple trajectories collected independently to estimate system parameters. Before algorithm design, the effect of multiplicative noise on moment dynamics is studied, and identifiability of the noise covariance matrix is clarified.

Taking the expectation of both sides of System (1) and denoting $\mu_t := \mathbb{E}\{x_t\}$ and $\nu_t := \mathbb{E}\{u_t\}$ yield the first-moment dynamic of system states (i.e., the dynamic of $\mathbb{E}\{x_t\}$) as follows,

$$\mu_{t+1} = A\mu_t + B\nu_t, \ t \in \mathbb{N}. \tag{3}$$

Denote the vectorization of the second-moment matrices of state, state-input, and input at time t by $X_t := \mathrm{vec}(\mathbb{E}\{x_t x_t^\mathsf{T}\})$, $W_t := \mathrm{vec}(\mathbb{E}\{x_t u_t^\mathsf{T}\})$, $W_t' := \mathrm{vec}(\mathbb{E}\{u_t x_t^\mathsf{T}\})$, and $U_t := \mathrm{vec}(\mathbb{E}\{u_t u_t^\mathsf{T}\})$. From the independence of $\bar{A}_t$ and $\bar{B}_t$, as well as vectorization, the second-moment dynamic of system states is

$$\begin{aligned} X_{t+1} &= (A\otimes A)X_t + (B\otimes A)W_t + (A\otimes B)W_t' \\ &\quad + (B\otimes B)U_t + \mathbb{E}\{(\bar{A}_t\otimes\bar{A}_t)\,\mathrm{vec}(x_t x_t^\mathsf{T})\} \\ &\quad + \mathbb{E}\{(\bar{B}_t\otimes\bar{B}_t)\,\mathrm{vec}(u_t u_t^\mathsf{T})\} \\ &= (A\otimes A + \Sigma_A')X_t + (B\otimes B + \Sigma_B')U_t \\ &\quad + (B\otimes A)W_t + (A\otimes B)W_t', \ t\in\mathbb{N}, \end{aligned} \tag{4}$$

where $\Sigma_A' = \mathbb{E}\{\bar{A}_t\otimes\bar{A}_t\} \in \mathbb{R}^{n^2\times n^2}$ and $\Sigma_B' = \mathbb{E}\{\bar{B}_t\otimes\bar{B}_t\} \in \mathbb{R}^{n^2\times m^2}$. The relation between (Σ_A, Σ_B) and (Σ_A', Σ_B') can be illustrated by $F(\Sigma_A', n, n, n, n) = \Sigma_A$ and $F(\Sigma_B', n, m, n, m) = \Sigma_B$, where the reshaping operator $F(\cdot)$ is defined in the notation section.

An intrinsic identifiability issue arises in the second-moment dynamic (4). Since $\mathbb{E}\{x_t x_t^\mathsf{T}\}$ is symmetric, X_t has $n(n-1)/2$ pairs of identical entries corresponding to the off-diagonal entries of $\mathbb{E}\{x_t x_t^\mathsf{T}\}$ (i.e., $\mathbb{E}\{x_{t,i}x_{t,j}\} = \mathbb{E}\{x_{t,j}x_{t,i}\}$ for all $i,j\in[n]$). To remove the redundant terms, introduce binary row- and column-selection matrices, which are also called elimination and duplication matrices (Magnus & Neudecker, 1980).

To begin, notice that the redundant entries of X_t are associated with the index set $\{(j-1)n+i : i,j\in[n], i<j\}$. Define matrix $T_1 \in \mathbb{R}^{n^2\times n^2}$ by replacing the $[(j-1)n+i]$th row of I_{n^2} by $(\mathbf{e}^{n^2}_{(i-1)n+j})^\mathsf{T}$ for all $i,j\in[n]$ with $i<j$. Note that $\mathbb{E}\{x_{t,i}x_{t,j}\}$ is the $[(j-1)n+i]$th entry of X_t, so X_t is invariant under T_1 (i.e., $X_t = T_1X_t$). Furthermore, define a binary elimination matrix P_1 that picks out only the unique entries of X_t, and a complementary binary duplication matrix Q_1 which in turn reconstructs X_t from the unique representation, by repeating the redundant entries in the proper order. These matrices are defined explicitly as $P_1 \in \mathbb{R}^{[n(n+1)/2]\times n^2}$ by removing the $[(j-1)n+i]$th row of I_{n^2}, $i,j\in[n]$ with $i<j$, and $Q_1 \in \mathbb{R}^{n^2\times[n(n+1)/2]}$ by removing the $[(j-1)n+i]$th column of T_1, $i,j\in[n]$ with $i<j$. Then one is able to freely convert between the full vectorization (with redundant entries) X_t and the symmetric vectorization (without redundant entries) $\tilde{X}_t := \mathrm{svec}(X_t)$, by employing the linear transformations defined by the matrices P_1 and Q_1:

$$\tilde{X}_t = P_1X_t, \qquad X_t = Q_1\tilde{X}_t.$$

Now apply the same arguments to the second moment of input U_t: U_t has $m(m-1)/2$ pairs of identical entries corresponding to the off-diagonal entries of $\mathbb{E}\{u_t u_t^\mathsf{T}\}$, so define $T_2 \in \mathbb{R}^{m^2\times m^2}$, $P_2 \in \mathbb{R}^{[m(m+1)/2]\times m^2}$, and $Q_2 \in \mathbb{R}^{m^2\times[m(m+1)/2]}$ by replacing n by m in the definitions of T_1, P_1, and Q_1, respectively.

Applying the symmetric vectorization transformations $\tilde{X}_t = P_1X_t$ and $\tilde{U}_t = P_2U_t$ yields the second-moment dynamic with unique entries,

$$\begin{aligned} \tilde{X}_{t+1} &= P_1X_{t+1} \\ &= P_1(A\otimes A + \Sigma_A')X_t + P_1(B\otimes B + \Sigma_B')U_t \\ &\quad + P_1(B\otimes A)W_t + P_1(A\otimes B)W_t' \\ &= P_1(A\otimes A + \Sigma_A')Q_1P_1X_t + P_1(B\otimes B + \Sigma_B')Q_2P_2U_t \\ &\quad + P_1(B\otimes A)W_t + P_1(A\otimes B)W_t' \\ &= (\tilde{A} + \tilde{\Sigma}_A')\tilde{X}_t + (\tilde{B} + \tilde{\Sigma}_B')\tilde{U}_t + K_{BA}W_t + K_{AB}W_t', \end{aligned} \tag{5}$$

where the penultimate equation follows from $T_1 = Q_1P_1$ and $T_2 = Q_2P_2$. In the last equation the following notations are introduced:

$$\begin{aligned} \tilde{A} &:= P_1(A\otimes A)Q_1 \in \mathbb{R}^{[n(n+1)/2]\times[n(n+1)/2]}, \\ \tilde{\Sigma}_A' &:= P_1\Sigma_A'Q_1 \in \mathbb{R}^{[n(n+1)/2]\times[n(n+1)/2]}, \\ \tilde{B} &:= P_1(B\otimes B)Q_2 \in \mathbb{R}^{[n(n+1)/2]\times[m(m+1)/2]}, \\ \tilde{\Sigma}_B' &:= P_1\Sigma_B'Q_2 \in \mathbb{R}^{[n(n+1)/2]\times[m(m+1)/2]}, \\ K_{BA} &:= P_1(B\otimes A), \ K_{AB} := P_1(A\otimes B). \end{aligned}$$

Note that $\tilde{X}_t$ and $\tilde{U}_t$ have no redundant entries but are able to capture the second-moment dynamic of system states. Let $[\bar{A}_t]_{ij}$ (resp. $[\bar{B}_t]_{ip}$) denote the (i,j)th entry of $\bar{A}_t$ (resp. (i,p)th entry of $\bar{B}_t$). The following proposition demonstrates the correspondences between the entries of $\tilde{\Sigma}_A'$ and $\tilde{\Sigma}_B'$ and those of Σ_A' and Σ_B', respectively.

Proposition 1. *Denote the (i,j)th entry of $\tilde{\Sigma}_A'$ by $[\tilde{\Sigma}_A']_{ij}$. It holds for $i,j,k,l\in[n]$ with $i<j$ and $k<l$ that*

$$\begin{aligned} &[\tilde{\Sigma}_A']_{(i-1)(n-i/2)+i,(k-1)(n-k/2)+k} = \mathbb{E}\{[\bar{A}_t]_{ik}[\bar{A}_t]_{ik}\}, \\ &[\tilde{\Sigma}_A']_{(i-1)(n-i/2)+i,(k-1)(n-k/2)+l} = 2\mathbb{E}\{[\bar{A}_t]_{ik}[\bar{A}_t]_{il}\}, \\ &[\tilde{\Sigma}_A']_{(i-1)(n-i/2)+j,(k-1)(n-k/2)+k} = \mathbb{E}\{[\bar{A}_t]_{ik}[\bar{A}_t]_{jk}\}, \\ &[\tilde{\Sigma}_A']_{(i-1)(n-i/2)+j,(k-1)(n-k/2)+l} \\ &\qquad = \mathbb{E}\{[\bar{A}_t]_{ik}[\bar{A}_t]_{jl}\} + \mathbb{E}\{[\bar{A}_t]_{il}[\bar{A}_t]_{jk}\}. \end{aligned}$$

Denote the (i,j)th entry of $\tilde{\Sigma}_B'$ by $[\tilde{\Sigma}_B']_{ij}$. It holds for $i,j\in[n]$ with $i<j$ and $p,q\in[m]$ with $p<q$ that

$$\begin{aligned} &[\tilde{\Sigma}_B']_{(i-1)(n-i/2)+i,(p-1)(m-p/2)+p} = \mathbb{E}\{[\bar{B}_t]_{ip}[\bar{B}_t]_{ip}\}, \\ &[\tilde{\Sigma}_B']_{(i-1)(n-i/2)+i,(p-1)(m-p/2)+q} = 2\mathbb{E}\{[\bar{B}_t]_{ip}[\bar{B}_t]_{iq}\}, \\ &[\tilde{\Sigma}_B']_{(i-1)(n-i/2)+j,(p-1)(m-p/2)+p} = \mathbb{E}\{[\bar{B}_t]_{ip}[\bar{B}_t]_{jp}\}, \\ &[\tilde{\Sigma}_B']_{(i-1)(n-i/2)+j,(p-1)(m-p/2)+q} \\ &\qquad = \mathbb{E}\{[\bar{B}_t]_{ip}[\bar{B}_t]_{jq}\} + \mathbb{E}\{[\bar{B}_t]_{iq}[\bar{B}_t]_{jp}\}. \end{aligned}$$

Remark 1. The preceding discussion indicates that X_t is determined by $[A\ B]$ and $[\tilde{\Sigma}_A'\ \tilde{\Sigma}_B']$, and the proposition shows that there exists a set of equivalent covariance matrices in the sense that they generate the same second-moment dynamic of system states, given the nominal matrix $[A\ B]$. This fact results from that the dynamic of $X_t = Q_1\tilde{X}_t$ only depends on $[A\ B]$ and $[\tilde{\Sigma}_A'\ \tilde{\Sigma}_B']$, and is the same under all (Σ_1', Σ_2') satisfying $P_1\Sigma_1'Q_1 = \tilde{\Sigma}_A'$ and $P_2\Sigma_2'Q_2 = \tilde{\Sigma}_B'$.

From an entry-wise point of view, $\mathbb{E}\{[\bar{A}_t]_{ik}[\bar{A}_t]_{jl}\}$ and $\mathbb{E}\{[\bar{A}_t]_{il}[\bar{A}_t]_{jk}\}$, $i\neq j$ and $k\neq l$, have a coupled effect on the second-moment dynamic of system states. We may only estimate the sum of these two entries out of X_t, rather than their exact values, since realizations of $\bar{A}_t$ and $\bar{B}_t$ are not observed directly but indirectly through their effect on system states. Fortunately, some entries of Σ_A' and Σ_B' are identifiable, such as $\mathbb{E}\{[\bar{A}_t]_{ik}[\bar{A}_t]_{ik}\}$, the variance of $[\bar{A}_t]_{ik}$, and $\mathbb{E}\{[\bar{A}_t]_{ik}[\bar{A}_t]_{jk}\}$, the covariance between entries in the same column. Similar issues

also appear, when estimating covariance matrices, in topics such as Kalman filtering (Mehra, 1970; Moghe et al., 2019). Critically, since these identifiable quantities uniquely generate the second-moment dynamic of system states, it suffices to estimate $\tilde{\Sigma}'_A$ and $\tilde{\Sigma}'_B$ for LQR design. This fact can be verified by expanding the Bellman equation; we omit the details to keep the paper concise.

Given (Σ_A, Σ_B) with $\Sigma_A \succeq 0$ and $\Sigma_B \succeq 0$ (then $\tilde{\Sigma}'_A = P_1 \Sigma'_A Q_1$ and $\tilde{\Sigma}'_B = P_2 \Sigma'_B Q_2$), the set of equivalent matrices discussed in Remark 1 can be written explicitly as follows, where positive semidefinite conditions are imposed because Σ_A and Σ_B are covariance matrices,

$$S^*(\tilde{\Sigma}'_A) := \Big\{ \Sigma_A(\alpha) \in \mathbb{R}^{n^2\times n^2} : \Sigma_A(\alpha) \succeq 0, \alpha \in \mathbb{R}^{n^2(n-1)^2/4} \Big\},$$

$$S^*(\tilde{\Sigma}'_B) := \Big\{ \Sigma_B(\beta) \in \mathbb{R}^{nm\times nm} : \Sigma_B(\beta) \succeq 0, \beta \in \mathbb{R}^{nm(n-1)(m-1)/4} \Big\},$$

$$S^*_\Sigma := S^*(\tilde{\Sigma}'_A) \times S^*(\tilde{\Sigma}'_B), \tag{6}$$

with $\Sigma_A(\alpha) := F(Q_1 \tilde{\Sigma}'_A Q_1^\intercal D_n + E_\alpha, n, n, n, n)$ and $\Sigma_B(\beta) := F(Q_1 \tilde{\Sigma}'_B Q_2^\intercal D_m + E_\beta, n, m, n, m)$. Here

$$E_\alpha = \sum_{\substack{i,j,k,l\in[n]\\ i<j,k<l}} \left[\alpha_{ij,kl} \left(\mathbf{e}^{n^2}_{(i-1)n+j} - \mathbf{e}^{n^2}_{(j-1)n+i} \right) \left(\mathbf{e}^{n^2}_{(k-1)n+l} - \mathbf{e}^{n^2}_{(l-1)n+k} \right)^\intercal \right],$$

$$E_\beta = \sum_{\substack{i,j\in[n],i<j\\ p,q\in[m],p<q}} \left[\beta_{ij,pq} \left(\mathbf{e}^{n^2}_{(i-1)n+j} - \mathbf{e}^{n^2}_{(j-1)n+i} \right) \left(\mathbf{e}^{m^2}_{(p-1)m+q} - \mathbf{e}^{m^2}_{(q-1)m+p} \right)^\intercal \right],$$

where $\alpha = [\alpha_{ij,kl}] \in \mathbb{R}^{n^2(n-1)^2/4}$, $\beta = [\beta_{ij,pq}] \in \mathbb{R}^{nm(n-1)(m-1)/4}$, $i, j, k, l \in [n]$, $p, q \in [m]$, $i < j$, $k < l$, $p < q$, Q_1 and Q_2 are given before (5), D_n is an n^2-dimensional diagonal matrix with $[(i-1)n+i]$th diagonal entry being 1 and the rest being $1/2$, $i \in [n]$, and D_m is an m^2-dimensional diagonal matrix with $[(p-1)m+p]$th diagonal entry being 1 and the rest being $1/2$, $p \in [m]$. Note that S^*_Σ is given by two inequalities which respectively depend on α and β. These two inequalities are linear matrix inequalities (Boyd et al., 1994), since the reshaping operator F is linear. Obviously S^*_Σ is not empty, because (Σ_A, Σ_B) is one of its elements. The following example provides an intuitive idea of previous discussions.

Example 1. Consider System (1) with $n = 2$ and $m = 1$, where $X_t = [\mathbb{E}\{x_{t,1}x_{t,1}\}\ \mathbb{E}\{x_{t,2}x_{t,1}\}\ \mathbb{E}\{x_{t,1}x_{t,2}\}\ \mathbb{E}\{x_{t,2}x_{t,2}\}]^T$. So $\mathbb{E}\{X_{t,2}X_{t,1}\}$ and $\mathbb{E}\{X_{t,1}X_{t,2}\}$ are identical and have the same dynamic from (4). Thus,

$$\tilde{X}_t = \begin{bmatrix} \mathbb{E}\{x_{t,1}x_{t,1}\} & \mathbb{E}\{x_{t,2}x_{t,1}\} & \mathbb{E}\{x_{t,2}x_{t,2}\} \end{bmatrix}^T,$$

$$P_1 = \begin{bmatrix} 1 & 0 & 0 & 0 \\ 0 & 1 & 0 & 0 \\ 0 & 0 & 0 & 1 \end{bmatrix},\ Q_1 = \begin{bmatrix} 1 & 0 & 0 \\ 0 & 1 & 0 \\ 0 & 1 & 0 \\ 0 & 0 & 1 \end{bmatrix},$$

$$T_1 = \begin{bmatrix} 1 & 0 & 0 & 0 \\ 0 & 1 & 0 & 0 \\ 0 & 1 & 0 & 0 \\ 0 & 0 & 0 & 1 \end{bmatrix},$$

$P_2 = Q_2 = T_2 = 1$.

According to the previously discussed simplification, we have that

$$\tilde{\Sigma}'_A = \begin{bmatrix} \sigma_{a,11,11} & 2\sigma_{a,11,12} & \sigma_{a,12,12} \\ \sigma_{a,11,21} & \sigma_{a,11,22} + \sigma_{a,12,21} & \sigma_{a,12,22} \\ \sigma_{a,21,21} & 2\sigma_{a,21,22} & \sigma_{a,22,22} \end{bmatrix},$$

$$\tilde{\Sigma}'_B = \begin{bmatrix} \sigma_{b,11} & \sigma_{b,12} & \sigma_{b,22} \end{bmatrix}^T,$$

where $\sigma_{a,ij,kl} = \mathbb{E}\{[\bar{A}_t]_{ij}[\bar{A}_t]_{kl}\}$, $\sigma_{b,ij} = \mathbb{E}\{[\bar{B}_t]_i, [\bar{B}_t]_j\}$. In this example, Σ_B is unique, but based on (6) the covariance matrix $\Sigma_A(\alpha)$, equivalent to Σ_A, is given by

$$\begin{bmatrix} \sigma_{a,11,11} & \sigma_{a,11,21} & \sigma_{a,11,12} & \sigma_{a,11,22} + \alpha \\ \sigma_{a,21,11} & \sigma_{a,21,21} & \sigma_{a,21,12} - \alpha & \sigma_{a,21,22} \\ \sigma_{a,12,11} & \sigma_{a,12,21} - \alpha & \sigma_{a,12,12} & \sigma_{a,12,22} \\ \sigma_{a,22,11} + \alpha & \sigma_{a,22,21} & \sigma_{a,22,12} & \sigma_{a,22,22} \end{bmatrix},$$

where $\alpha \in \mathbb{R}$ is such that $\Sigma_A(\alpha) \succeq 0$.

As shown in Example 1, given (Σ_A, Σ_B) with $\Sigma_A \succeq 0$ and $\Sigma_B \succeq 0$, the set S^*_Σ is not empty but may have infinitely many elements, resulting in unidentifiable entries $\mathbb{E}\{[\bar{A}_t]_{ik}[\bar{A}_t]_{jl}\}$ and $\mathbb{E}\{[\bar{B}_t]_{ip}[\bar{B}_t]_{jq}\}$, $i \neq j$, $k \neq l$, $p \neq q$, $i, j, k, l \in [n]$, $p, q \in [m]$. The following proposition gives several conditions under which the covariance matrix of the multiplicative noise can or cannot be uniquely determined from $[\tilde{\Sigma}'_A\ \tilde{\Sigma}'_B]$.

Proposition 2. *Given (Σ_A, Σ_B) with $\Sigma_A \succeq 0$ and $\Sigma_B \succeq 0$, $\tilde{\Sigma}'_A = P_1 \Sigma'_A Q_1$ and $\tilde{\Sigma}'_B = P_2 \Sigma'_B Q_2$, the following results hold.*
(i) If $n = m = 1$, then S^*_Σ has a unique element. If $m = 1$, then $S^*(\tilde{\Sigma}'_B)$ has a unique element. If $n \geq 2$ and $\Sigma_A \succ 0$ (resp. $m \geq 2$ and $\Sigma_B \succ 0$), then $S^*(\tilde{\Sigma}'_A)$ (resp. $S^*(\tilde{\Sigma}'_B)$) has infinitely many elements. As a result, under either condition, S^*_Σ has infinitely many elements.
(ii) If $S^*(\tilde{\Sigma}'_A)$ has infinitely many elements, then $S^*(\tilde{\Sigma}'_A) \cap T_A$ has a unique element, where

$$T_A := \{\Sigma \in \mathbb{R}^{n^2\times n^2} : \gamma_{ij,kl}\Sigma_{(k-1)n+i,(l-1)n+j} + \delta_{ij,kl}\Sigma_{(l-1)n+i,(k-1)n+j} = \tau_{ij,kl}, i < j, k < l, i, j, k, l \in [n]\},$$

with constants $\gamma_{ij,kl}, \delta_{ij,kl}, \tau_{ij,kl} \in \mathbb{R}$ and $\gamma_{ij,kl} \neq \delta_{ij,kl}$ for all $i < j$, $k < l$, $i, j, k, l \in [n]$. The same result holds for $S^*(\tilde{\Sigma}'_B)$ by modifying the definition of T_A according to the dimension of Σ_B.

Remark 2. The first part of the proposition shows that if $\Sigma_A \succ 0$ or $\Sigma_B \succ 0$ and $n \geq m \geq 2$, then it is impossible to uniquely determine (Σ_A, Σ_B) only based on the second-moment dynamic (5). However the second part indicates that more conditions imposed on the covariance matrix can make all entries of Σ_A and Σ_B identifiable. The set T_A introduces additional constraints for $\mathbb{E}\{[\bar{A}_t]_{ik}[\bar{A}_t]_{jl}\}$, $i \neq j$, $k \neq l$. For example, if entries in $\bar{A}_t$ are mutually independent, then Σ_A is diagonal. In this case, it holds that $\mathbb{E}\{[\bar{A}_t]_{ik}[\bar{A}_t]_{jl}\} - \mathbb{E}\{[\bar{A}_t]_{il}[\bar{A}_t]_{jk}\} = 0$, $i \neq j$, $k \neq l$, and hence the covariance matrix of $\bar{A}_t$ is uniquely determined.

Now we are ready to propose our estimation algorithm. Following the previous discussion, we introduce an algorithm based on the first- and second-moment dynamics (3) and (5). Since the exact moment dynamics are unavailable, we average over multiple independent rollouts to obtain their estimates. To get persistently exciting inputs, it is necessary to design their first and second moments in advance, in either a deterministic or a stochastic way. For example, generate the two moments from standard Gaussian and Wishart distributions (Gupta & Nagar, 2018), respectively, or set them periodically. The initial states of different

Algorithm 1
Multiple-trajectory averaging least-squares (MALS)

Input: Rollout length ℓ and number of rollouts n_r.
Output: $[\hat{A}\ \hat{B}]$, $[\hat{\tilde{\Sigma}}'_A\ \hat{\tilde{\Sigma}}'_B]$.
// **Control-input design**
1: **for** t from 0 to $\ell-1$ **do**
2: Generate $\nu_t \in \mathbb{R}^m$ and $\bar{U}_t \in \mathbb{R}^{m\times m}$ with $\bar{U}_t \succeq 0$.
3: **end for**
// **Multiple-trajectory collection**
4: **for** k from 1 to n_r **do**
5: Generate $x_0^{(k)}$ independently from the initial multivariate distribution $\mathcal{X}_0$.
6: **for** t from 0 to $\ell-1$ **do**
7: Generate $u_t^{(k)}$ independently from a multivariate distribution with first moment ν_t and second central moment $\bar{U}_t$,
8: $x_{t+1}^{(k)} = (A+\bar{A}_t^{(k)})x_t^{(k)} + (B+\bar{B}_t^{(k)})u_t^{(k)}$.
9: **end for**
10: **end for**
// **Least-squares estimation**
11: **for** t from 0 to ℓ **do**
12: Compute

$$\hat{\mu}_t := \frac{1}{n_r}\sum_{k=1}^{n_r} x_t^{(k)},$$

$$\hat{\tilde{X}}_t := \frac{1}{n_r} P_1 \operatorname{vec}\left(\sum_{k=1}^{n_r} x_t^{(k)}(x_t^{(k)})^\intercal\right),$$

$$\hat{W}_t := \frac{1}{n_r}\operatorname{vec}\left(\sum_{k=1}^{n_r} x_t^{(k)}\nu_t^\intercal\right) = \operatorname{vec}(\hat{\mu}_t\nu_t^\intercal),$$

$$\hat{W}'_t := \frac{1}{n_r}\operatorname{vec}\left(\sum_{k=1}^{n_r} \nu_t x_t^{(k)\intercal}\right) = \operatorname{vec}(\nu_t\hat{\mu}_t^\intercal),$$

$$\tilde{U}_t := P_2\operatorname{vec}(\bar{U}_t + \nu_t\nu_t^\intercal).$$

13: **end for**
14: $[\hat{A}\ \hat{B}] = \underset{[A\ B]}{\operatorname{argmin}}\{\sum_{t=0}^{\ell-1}\|\hat{\mu}_{t+1} - (A\hat{\mu}_t + B\nu_t)\|_2^2\}$,
15: Compute $\hat{\tilde{A}} = P_1(\hat{A}\otimes\hat{A})Q_1$, $\hat{\tilde{B}} = P_1(\hat{B}\otimes\hat{B})Q_2$, $\hat{K}_{BA} = P_1(\hat{B}\otimes\hat{A})$, and $\hat{K}_{AB} = P_1(\hat{A}\otimes\hat{B})$, where P_1, P_2, Q_1, and Q_2 are given before (5),
16: $[\hat{\tilde{\Sigma}}'_A\ \hat{\tilde{\Sigma}}'_B] = \underset{[\tilde{\Sigma}'_A\ \tilde{\Sigma}'_B]}{\operatorname{argmin}}\{\sum_{t=0}^{\ell-1}\|\hat{\tilde{X}}_{t+1} - [\tilde{A}\hat{\tilde{X}}_t + K_{BA}\hat{W}_t + K_{AB}\hat{W}'_t + \tilde{B}\tilde{U}_t + \tilde{\Sigma}'_A\hat{\tilde{X}}_t + \tilde{\Sigma}'_B\tilde{U}_t]\|_2^2\}$.

rollouts are assumed to be i.i.d. subject to a same distribution $\mathcal{X}_0$ with finite second moment (see Section 3.2.2). The overall algorithm is shown in Algorithm 1, where the superscript (k) represents the kth rollout. Note that Algorithm 1 is different from classic recursive identification algorithms. The recursive least-squares algorithm (Chen & Guo, 2012; Lai & Wei, 1982), for example, uses only one trajectory of a system. In contrast, Algorithm 1 is based on multiple trajectories with finite length.

Based on the estimates $\hat{\tilde{\Sigma}}'_A$ and $\hat{\tilde{\Sigma}}'_B$, it is able to obtain an estimate $\hat{S}^*_\Sigma$ of the equivalent class (6), via replacing $\tilde{\Sigma}'_A$ and $\tilde{\Sigma}'_B$ in the definition (6) by their estimates. If the linear matrix inequalities are infeasible (i.e., $\hat{S}^*_\Sigma = \emptyset$), then project the estimates onto the positive semidefinite cone. However this situation is unlikely to happen when n_r is large, because of the consistency of Algorithm 1 given in the next section.

3.2. Performance of Algorithm 1

This section analyzes performance of Algorithm 1 by investigating the moment dynamics (3) and (5).

3.2.1. Moment dynamics and input design

Provided that μ_t and $\tilde{X}_t$ are known, it is possible to recover the parameters via least-squares as in lines 14 – 16 in Algorithm 1. Denote

$$\mathbf{Y} := [\mu_\ell\ \cdots\ \mu_1],\ \mathbf{Z} := \begin{bmatrix}\mu_{\ell-1} & \cdots & \mu_0\\ \nu_{\ell-1} & \cdots & \nu_0\end{bmatrix},$$
$$\mathbf{C} := [C_\ell\ \cdots\ C_1],\ \mathbf{D} := \begin{bmatrix}\tilde{X}_{\ell-1} & \cdots & \tilde{X}_0\\ \tilde{U}_{\ell-1} & \cdots & \tilde{U}_0\end{bmatrix}, \tag{7}$$

where $C_t = \tilde{X}_t - \left(\tilde{A}\tilde{X}_{t-1} + K_{BA}W_{t-1} + K_{AB}W'_{t-1} + \tilde{B}\tilde{U}_{t-1}\right)$, $1 \le t \le \ell$. Then closed-form solutions of the least-squares problems are

$$\left[\hat{A}\ \hat{B}\right] = \mathbf{Y}\mathbf{Z}^\intercal(\mathbf{Z}\mathbf{Z}^\intercal)^\dagger,\ \left[\hat{\tilde{\Sigma}}'_A\ \hat{\tilde{\Sigma}}'_B\right] = \mathbf{C}\mathbf{D}^\intercal(\mathbf{D}\mathbf{D}^\intercal)^\dagger,$$

where $\dagger$ represents the pseudoinverse. When the inverse matrices exist, the solutions are identical to true values; that is, $[\hat{A}\ \hat{B}] = [A\ B]$ and $[\hat{\tilde{\Sigma}}'_A\ \hat{\tilde{\Sigma}}'_B] = [\tilde{\Sigma}'_A\ \tilde{\Sigma}'_B]$. Hence, the first question towards the consistency of Algorithm 1 is whether the matrices $\mathbf{Z}\mathbf{Z}^\intercal$ and $\mathbf{D}\mathbf{D}^\intercal$ are invertible. As to be shown, designing a proper input sequence ensures this invertibility, if systems (A, B) and $(\tilde{A} + \tilde{\Sigma}'_A, \tilde{B} + \tilde{\Sigma}'_B)$ are controllable, and the rollout length ℓ is large enough.

Proposition 3. *Suppose that $\ell \ge n+m$ and (A, B) is controllable. For fixed $\mu_0 \in \mathbb{R}^n$, the matrix $\mathbf{Z}$ has full row rank, and consequently $\mathbf{Z}\mathbf{Z}^\intercal$ is invertible, for almost all $[\nu_0^\intercal\ \cdots\ \nu_{\ell-1}^\intercal]^\intercal \in \mathbb{R}^{m\ell}$.*

Remark 3. The proposition shows that for large enough rollout length, the full row rankness of $\mathbf{Z}$ can be guaranteed for almost all $[\nu_0^\intercal\ \cdots\ \nu_{\ell-1}^\intercal]^\intercal \in \mathbb{R}^{m\ell}$. The controllability of (A, B) plays a key role in the proof, similar to classic results on identification of linear systems (Chen & Guo, 2012). The condition $\ell \ge n+m$ is necessary for the invertibility of $\mathbf{Z}\mathbf{Z}^\intercal$. This lower bound is much smaller than that given in Xing et al. (2020). According to the proposition, $\mathbf{Z}\mathbf{Z}^\intercal$ is invertible with probability one if the first moments of inputs are generated i.i.d. from a distribution absolutely continuous with respect to Lebesgue measure (e.g., Gaussian distribution or uniform distribution). This proposition can be seen as a generalization of the single-input case studied in Schmidt et al. (2005).

Proposition 4. *Suppose that $\ell \ge [n(n+1)+m(m+1)]/2$ and $(\tilde{A}+\tilde{\Sigma}'_A, \tilde{B}+\tilde{\Sigma}'_B)$ is controllable. For fixed $\mu_0 \in \mathbb{R}^n$ and $\tilde{X}_0 \in \mathbb{R}^{n(n+1)/2}$, the matrix $\mathbf{D}$ has full row rank, and consequently $\mathbf{D}\mathbf{D}^\intercal$ is invertible, for almost all $[\nu_0^\intercal\ \cdots\ \nu_{\ell-1}^\intercal\ \operatorname{svec}(\bar{U}_0)^\intercal\ \cdots\ \operatorname{svec}(\bar{U}_{\ell-1})^\intercal]^\intercal \in \mathbb{R}^{\ell m(m+3)/2}$, where $\bar{U}_t$ is defined in line 2 of Algorithm 1.*

Remark 4. The controllability condition in Proposition 4 reflects the nature of the multiplicative noise (i.e., coupling between $\bar{A}_t$ and x_t, and that between $\bar{B}_t$ and u_t). The result indicates that a controllability condition on (5) may be necessary to ensure successful identification. The lower bound for ℓ is necessary for the invertibility of $\mathbf{D}\mathbf{D}^\intercal$, and is much smaller than that given in Xing et al. (2020). As in Algorithm 1, $\tilde{U}_t = \operatorname{svec}(\bar{U}_t + \nu_t\nu_t^\intercal)$, so random generation of ν_t and $\bar{U}_t$ ensures that $\mathbf{D}\mathbf{D}^\intercal$ is invertible with probability one.

We summarize the preceding two results in the following corollary.

Corollary 1. *Suppose that $\ell \geq [n(n+1)+m(m+1)]/2$, and that both (A, B) and $(\tilde{A}+\tilde{\Sigma}'_A, \tilde{B}+\tilde{\Sigma}'_B)$ are controllable. For fixed $\mu_0 \in \mathbb{R}^n$ and $\tilde{X}_0 \in \mathbb{R}^{n(n+1)/2}$, the matrices $\mathbf{Z}\mathbf{Z}^\intercal$ and $\mathbf{D}\mathbf{D}^\intercal$ are invertible, for almost all $[\nu_0^\intercal \cdots \nu_{\ell-1}^\intercal \ \mathrm{svec}(\bar{U}_0)^\intercal \cdots \mathrm{svec}(\bar{U}_{\ell-1})^\intercal]^\intercal \in \mathbb{R}^{\ell m(m+3)/2}$, where $\bar{U}_t$ is defined in line 2 of Algorithm 1.*

Remark 5. The corollary implies that the existence of $(\mathbf{Z}\mathbf{Z}^\intercal)^{-1}$ and $(\mathbf{D}\mathbf{D}^\intercal)^{-1}$ can be guaranteed with probability one, as long as both ν_t and $\bar{U}_t$ are independently generated from distributions that are absolutely continuous with respect to Lebesgue measure. For example, the entries of ν_t are generated i.i.d. from a non-degenerate Gaussian distribution and then $\bar{U}_t$ is generated i.i.d. from a non-degenerate Wishart distribution, $0 \leq t \leq \ell-1$.

3.2.2. Asymptotic consistency

In this subsection, we assume that the expectations and covariance matrices of inputs have been generated as discussed in the previous section, and that both $\mathbf{Z}\mathbf{Z}^\intercal$ and $\mathbf{D}\mathbf{D}^\intercal$ have been designed to be invertible. The closed-form estimates generated by Algorithm 1 are

$$\begin{bmatrix}\hat{A} & \hat{B}\end{bmatrix} = \hat{\mathbf{Y}}\hat{\mathbf{Z}}^\intercal(\hat{\mathbf{Z}}\hat{\mathbf{Z}}^\intercal)^\dagger, \tag{8}$$

$$\begin{bmatrix}\hat{\tilde{\Sigma}}'_A & \hat{\tilde{\Sigma}}'_B\end{bmatrix} = \hat{\mathbf{C}}\hat{\mathbf{D}}^\intercal(\hat{\mathbf{D}}\hat{\mathbf{D}}^\intercal)^\dagger, \tag{9}$$

where

$$\hat{\mathbf{Y}} := \begin{bmatrix}\hat{\mu}_\ell & \cdots & \hat{\mu}_1\end{bmatrix}, \quad \hat{\mathbf{Z}} := \begin{bmatrix}\hat{\mu}_{\ell-1} & \cdots & \hat{\mu}_0 \\ \nu_{\ell-1} & \cdots & \nu_0\end{bmatrix}, \tag{10}$$

$$\hat{\mathbf{C}} := \begin{bmatrix}\hat{C}_\ell & \cdots & \hat{C}_1\end{bmatrix}, \quad \hat{\mathbf{D}} := \begin{bmatrix}\hat{\tilde{X}}_{\ell-1} & \cdots & \hat{\tilde{X}}_0 \\ \tilde{U}_{\ell-1} & \cdots & \tilde{U}_0\end{bmatrix}, \tag{11}$$

and $\hat{C}_t = \hat{\tilde{X}}_t - \big(\hat{\tilde{A}}\hat{\tilde{X}}_{t-1} + \hat{K}_{BA}\hat{W}_{t-1} + \hat{K}_{AB}\hat{W}'_{t-1} + \hat{\tilde{B}}\tilde{U}_{t-1}\big)$, $1 \leq t \leq \ell$. Here $\hat{\tilde{A}}$, $\hat{\tilde{B}}$, $\hat{K}_{AB}$, and $\hat{K}_{BA}$ are estimates of $\tilde{A}$, $\tilde{B}$, K_{AB}, and K_{BA}, obtained from $\hat{A}$ and $\hat{B}$ given by Algorithm 1. The estimates depend on the number of rollouts n_r, which is omitted for convenience. For the convergence result, we present the following assumptions.

Assumption 1. For all rollouts indexed by $k \in [n_r]$, the below conditions hold.
(i) The rollout length is $\ell \geq [n(n+1)+m(m+1)]/2$.
(ii) The initial states $x_0^{(k)}$, $k \in [n_r]$, are i.i.d. subject to the same distribution $\mathcal{X}_0$ with finite second moment, and are independent of the multiplicative noise and inputs.
(iii) $\{\bar{A}_t^{(k)}, 0 \leq t \leq \ell, k \in [n_r]\}$ and $\{\bar{B}_t^{(k)}, 0 \leq t \leq \ell, k \in [n_r]\}$, are i.i.d. sequences respectively and are mutually independent, both with zero mean and finite second moments (i.e., $\mathbb{E}\{\bar{A}_t^{(k)}\}$ and $\mathbb{E}\{\bar{B}_t^{(k)}\}$ are zero matrices, and $\|\Sigma_A\|_2, \|\Sigma_B\|_2 < \infty$).
(iv) The parameters of inputs are given by lines 1–3 of Algorithm 1, and the inputs are generated, according to line 7 of Algorithm 1. The inputs and noise are independent.
(v) Both $\mathbf{Z}\mathbf{Z}^\intercal$ and $\mathbf{D}\mathbf{D}^\intercal$ are invertible.

Remark 6. From Corollary 1, the lower bound of the rollout length in Assumption 1(i) is necessary for estimating the noise covariance matrix, whereas, from Proposition 3, trajectories with length $\ell \geq n+m$ may be enough for estimating the nominal system matrix. The initial states of different trajectories need not start with the same value, but it is required that they have the same first and second moments (Assumption 1(ii)). The mutual independence of noise at different time steps in one trajectory is a standard assumption (Assumption 1(iii)). The results in this paper still hold, if the noise sequence in the same trajectory is dependent, but the noise sequences in different trajectories are mutually independent and the noise has zero mean and the same second moment. The physical meaning of the independence between the noise and the inputs in Assumption 1(iv) is that the former is an intrinsic part of the system and cannot be influenced by inputs. To keep the analysis concise, we separately discuss the input design (Section 3.2.1) and performance of Algorithm 1. Assumption 1(v) indicates that the input design yields invertible $\mathbf{Z}\mathbf{Z}^\intercal$ and $\mathbf{D}\mathbf{D}^\intercal$, but note that this assumption implicitly assumes the controllability of the first- and second-moment dynamics of system states.

Under Assumption 1 the rollouts $[x_0^{(k)}, \ldots, x_l^{(k)}]$, $k \in [n_r]$, are i.i.d., so the following consistency result can be obtained from the strong law of large numbers.

Theorem 1 (*Consistency*)**.** *Suppose that Assumption 1 holds, then the estimators (8)–(9) are asymptotically consistent, namely,*

$$\begin{bmatrix}\hat{A} & \hat{B}\end{bmatrix} \to [A \ B] \quad \textit{and} \quad \begin{bmatrix}\hat{\tilde{\Sigma}}'_A & \hat{\tilde{\Sigma}}'_B\end{bmatrix} \to \begin{bmatrix}\tilde{\Sigma}'_A & \tilde{\Sigma}'_B\end{bmatrix},$$

with probability one as the number of rollouts $n_r \to \infty$.

Remark 7. This theorem indicates that consistency of Algorithm 1 may hold even when the rollout length is relatively small. In Di and Lamperski (2021), the estimation of the first and second moments of multiplicative noise is decoupled, whereas here the estimate of $[\tilde{\Sigma}'_A \ \tilde{\Sigma}'_B]$ relies on $[\hat{A} \ \hat{B}]$. The coupling exists because here the noise covariance matrix, which from definition depends on the mean of the noise, is estimated. Note that ℓ is assumed to be fixed and we do not consider the case where $\ell \to \infty$, since an averaging step is used in Algorithm 1. Study of the case with increasing rollout length is left to future work.

3.3. Finite-sample analysis

This subsection studies finite-sample performance of Algorithm 1, demonstrating its non-asymptotic behavior. The existence of multiplicative noise complicates the analysis, so the following assumptions, ensuring that the system is bounded a.s., are introduced.

Assumption 2. For all rollouts indexed by $k \in [n_r]$, the following conditions hold.
(i) The initial state is bounded a.s. for all $k \in [n_r]$ as

$$\|x_0^{(k)}\| \leq c_X < \infty.$$

(ii) The inputs are bounded a.s. for all $0 \leq t \leq \ell-1$ and $k \in [n_r]$ as

$$\|u_t^{(k)}\| \leq c_U < \infty.$$

(iii) The multiplicative noise, $\bar{A}_t^{(k)}$ and $\bar{B}_t^{(k)}$, is bounded a.s. for all $0 \leq t \leq \ell-1$ and $k \in [n_r]$ as

$$\|\bar{A}_t^{(k)}\|_2 \leq c_{\bar{A}} < \infty, \ \ \|\bar{B}_t^{(k)}\|_2 \leq c_{\bar{B}} < \infty.$$

Remark 8. The assumption of bounded multiplicative noise is reasonable for physical systems, which cannot have infinite variations. For example, in interconnected systems, the noise represents randomly varying topologies of subsystems, and is naturally bounded.

The following theorems state finite-sample results for the estimates of $[A \ B]$ and $[\tilde{\Sigma}'_A \ \tilde{\Sigma}'_B]$.

Theorem 2. *Suppose that Assumptions 1 and 2 hold. Fix a failure probability $\delta \in (0,1)$. It holds with probability at least $1-\delta$ that*

$$\left\|\begin{bmatrix}\hat{A} & \hat{B}\end{bmatrix} - [A \ B]\right\|_2 \leq \mathcal{O}\left(\sqrt{\frac{\ell \log(\ell/\delta)}{n_r}}\right).$$

Theorem 3. *Under the same condition of Theorem 2, with probability at least* $1-\delta$*, it holds that*

$$\left\|\begin{bmatrix}\hat{\tilde{\Sigma}}'_A & \hat{\tilde{\Sigma}}'_B\end{bmatrix}-\begin{bmatrix}\tilde{\Sigma}'_A & \tilde{\Sigma}'_B\end{bmatrix}\right\|_2 \le \mathcal{O}\left(\sqrt{\frac{\ell\log(\ell/\delta)}{n_r}}\right).$$

Remark 9. In Theorems 2 and 3, high-probability upper bounds are given for the estimates of $[A\ B]$ and $[\tilde{\Sigma}'_A\ \tilde{\Sigma}'_B]$. It can be observed that these bounds shrink as $\mathcal{O}\left(1/\sqrt{n_r}\right)$ with the number of rollouts, and converge to zero as the number of rollouts grows to infinity, indicating the consistency of the estimators. Note that the bounds are deterministic, although they depend on the failure probability δ. The theorems also indicate that the probability of the estimation error exceeding an arbitrary positive constant decays exponentially fast with the number of rollouts, which is illustrated in Section 4.1.

The $\mathcal{O}(\cdot)$ notation hides the coefficients of the error bounds, and the polynomial and exponential factors of n and m in the logarithm term. Their explicit forms are given in the extended version (Xing et al., 2021). The coefficient of the estimation error of $[A\ B]$ increases with $\|\mathbf{Y}\|_2$, $\|\mathbf{Z}\|_2$, and the bound of the system, but decreases with the minimum eigenvalue of $\mathbf{Z}\mathbf{Z}^\top$. Similarly, the coefficient of the estimation error of $[\tilde{\Sigma}'_A\ \tilde{\Sigma}'_B]$ decreases with the minimum eigenvalue of $\mathbf{D}\mathbf{D}^\top$, but increases with $\|\mathbf{C}\|_2$, $\|\mathbf{D}\|_2$, and the bound of the system. It also increases with $\|A\|_2$, $\|B\|_2$, and quantities related to the second-moment dynamic of system states, because of the dependence of $[\hat{\tilde{\Sigma}}'_A\ \hat{\tilde{\Sigma}}'_B]$ on $[\hat{A}\ \hat{B}]$. From definition, $\mathbf{Y}$, $\mathbf{Z}$, $\mathbf{C}$, and $\mathbf{D}$ depend on system parameters and inputs, so proper input design could reduce the estimation error. It remains for future study how to design the moments of inputs so that the coefficients of the bounds can achieve their smallest values, and how to obtain data-dependent bounds, because the nominal system matrix is unknown.

In Di and Lamperski (2021), the authors study identification of System (1) from single-trajectory data, by developing error bounds for a least-squares algorithm, but it is unclear under what conditions of System (1) these error bounds converge to zero. In contrast, our analysis provides sufficient conditions under which the error bounds for estimates given by Algorithm 1 vanish. The results show that a relatively small rollout length is enough to guarantee consistency, but the current bounds imply that longer rollout length ℓ may lead to worse performance, which seems to be contrary to the intuition that longer trajectory provides more information. This could result from the averaging step which eliminates some excitation. Future work will consider how to use the data more efficiently.

PROOF SKETCH. The detailed proofs of Theorems 2 and 3 can be found in Xing et al. (2021). Most parts are elementary, and omitted due to space limit. Here a proof sketch is provided. Note that the estimation error $[\hat{A}\ \hat{B}]-[A\ B]$ can be decomposed as

$$\begin{aligned}&\left[\hat{A}\ \hat{B}\right]-[A\ B]\\&=\hat{\mathbf{Y}}\hat{\mathbf{Z}}^\top(\hat{\mathbf{Z}}\hat{\mathbf{Z}}^\top)^\dagger-\mathbf{Y}\mathbf{Z}^\top(\mathbf{Z}\mathbf{Z}^\top)^{-1}\\&=\left[\hat{\mathbf{Y}}\hat{\mathbf{Z}}^\top-\mathbf{Y}\mathbf{Z}^\top\right](\mathbf{Z}\mathbf{Z}^\top)^{-1}+\mathbf{Y}\mathbf{Z}^\top\left[(\hat{\mathbf{Z}}\hat{\mathbf{Z}}^\top)^\dagger-(\mathbf{Z}\mathbf{Z}^\top)^{-1}\right]\\&\quad+\left[\hat{\mathbf{Y}}\hat{\mathbf{Z}}^\top-\mathbf{Y}\mathbf{Z}^\top\right]\left[(\hat{\mathbf{Z}}\hat{\mathbf{Z}}^\top)^\dagger-(\mathbf{Z}\mathbf{Z}^\top)^{-1}\right].\end{aligned}$$

Because $\hat{\mathbf{Y}}-\mathbf{Y}$ and $\hat{\mathbf{Z}}-\mathbf{Z}$ are sums of zero-mean independent random matrices (by definition), a matrix Bernstein inequality (Tropp, 2015) gives bounds for the spectral norms of $\hat{\mathbf{Y}}-\mathbf{Y}$ and $\hat{\mathbf{Z}}-\mathbf{Z}$. Given these two bounds, we analyze $\|\hat{\mathbf{Y}}\hat{\mathbf{Z}}^\top-\mathbf{Y}\mathbf{Z}^\top\|_2$ and $\|\hat{\mathbf{Z}}\hat{\mathbf{Z}}^\top-\mathbf{Z}\mathbf{Z}^\top\|_2$.

Next, an ε-net argument provides an upper bound for the maximum eigenvalue of $\hat{\mathbf{Z}}\hat{\mathbf{Z}}^\top$ and a lower bound for the minimum eigenvalue of $\hat{\mathbf{Z}}\hat{\mathbf{Z}}^\top$. The latter is with high probability close to the minimum eigenvalue of $\mathbf{Z}\mathbf{Z}^\top$. This fact implies that $(\hat{\mathbf{Z}}\hat{\mathbf{Z}}^\top)^{-1}$ exists with high probability, since $\mathbf{Z}\mathbf{Z}^\top$ is invertible from Assumption 1(v). Hence, from the inequality,

$$\begin{aligned}&\left\|(\hat{\mathbf{Z}}\hat{\mathbf{Z}}^\top)^{-1}-(\mathbf{Z}\mathbf{Z}^\top)^{-1}\right\|_2\\&\le\left\|(\mathbf{Z}\mathbf{Z}^\top)^{-1}\right\|_2\left\|(\hat{\mathbf{Z}}\hat{\mathbf{Z}}^\top)^{-1}\right\|_2\left\|\hat{\mathbf{Z}}\hat{\mathbf{Z}}^\top-\mathbf{Z}\mathbf{Z}^\top\right\|_2,\end{aligned}$$

it follows that the spectral norm of $(\hat{\mathbf{Z}}\hat{\mathbf{Z}}^\top)^\dagger-(\mathbf{Z}\mathbf{Z}^\top)^{-1}$ can be upper bounded by $\|\hat{\mathbf{Z}}\hat{\mathbf{Z}}^\top-\mathbf{Z}\mathbf{Z}^\top\|_2$ with high probability.

Finally, a union bound combining the preceding results yields the conclusion. The probability bound for the estimate error of the noise covariance matrix can be obtained in a similar way. □

4. Numerical simulations

In this section we empirically validate the theoretical results for Algorithm 1, and compare its performance with the recursive least-squares algorithm based on single-trajectory data (Chen & Guo, 2012; Lai & Wei, 1982).

4.1. Consistency and finite-sample result

This subsection considers identification of the 2-dimensional system discussed in Example 1 with parameters

$$A=\begin{bmatrix}1&0.2\\0&1\end{bmatrix},\ B=\begin{bmatrix}0.8\\1\end{bmatrix},$$

$$\Sigma_A=\frac{1}{40}\begin{bmatrix}8&-2&0&0\\-2&16&2&0\\0&2&2&0\\0&0&0&8\end{bmatrix},\ \Sigma_B=\frac{1}{40}\begin{bmatrix}5&-2\\-2&20\end{bmatrix}.$$

According to the reshaping operator G defined in the notation section and the discussion in Example 1, it holds that

$$\tilde{\Sigma}'_A=\frac{1}{40}\begin{bmatrix}8&0&2\\-2&2&0\\16&0&8\end{bmatrix},\ \tilde{\Sigma}'_B=\frac{1}{40}\begin{bmatrix}5&-2&20\end{bmatrix}^\top. \tag{12}$$

A simulated experiment is conducted with rollout data of length $\ell=4$. For $0\le t\le 3$, ν_t is generated independently from uniform distribution $\mathcal{U}([0,1])$ and then fixed. Three types of inputs are considered: Gaussian, uniform, and deterministic inputs. An identical sequence of input covariances, independently generated from 1-dimensional Wishart distribution $W_p(0.1,1)$ and then fixed, is used in the former two cases. For the case of deterministic inputs, the covariances are set to be zero (i.e., $\bar{U}_t=0$). In this setting $\mathbf{D}\mathbf{D}^\top$ can be invertible because the second moment of the input at time t satisfies that $U_t=\bar{U}_t+\nu_t\nu_t^\top$, and the generation of ν_t provides randomness. For each case, Algorithm 1 is run for 50 times. The mean of estimation error in each case is shown in Fig. 1. It can be seen that Algorithm 1 converges with convergence rate $\mathcal{O}(1/\sqrt{n_r})$, and performs similarly under all three types of inputs. The algorithm fluctuates when the number of rollouts is small, which may result from the averaging step.

Fig. 2 provides the relative frequency of the normalized estimation errors, $\|[\hat{A}\ \hat{B}]-[A\ B]\|_2/\|[A\ B]\|_2$ and $\|[\hat{\tilde{\Sigma}}'_A\ \hat{\tilde{\Sigma}}'_B]-[\tilde{\Sigma}'_A\ \tilde{\Sigma}'_B]\|_2/\|[\tilde{\Sigma}'_A\ \tilde{\Sigma}'_B]\|_2$, exceeding a given constant, under the uniform-input case. This result shows an exponential decay of the frequency and validates the finite-sample results. The relative frequency of n_r rollouts is denoted by p_{n_r}.

From Remark 1 and (6), it follows that (12) defines an equivalent class of covariance matrices that generates the same second-moment dynamic of system states. In the current example, Σ_B is

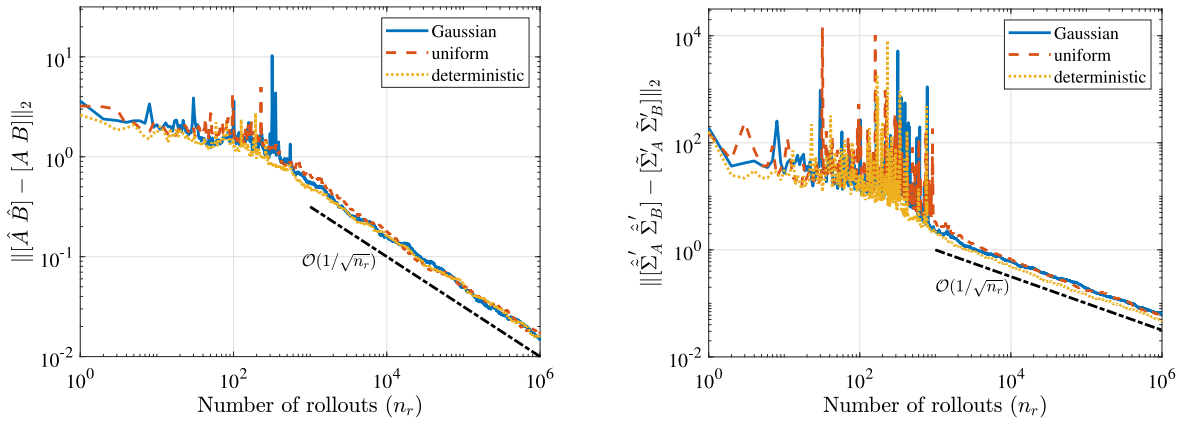

Fig. 1. Consistency of Algorithm 1.

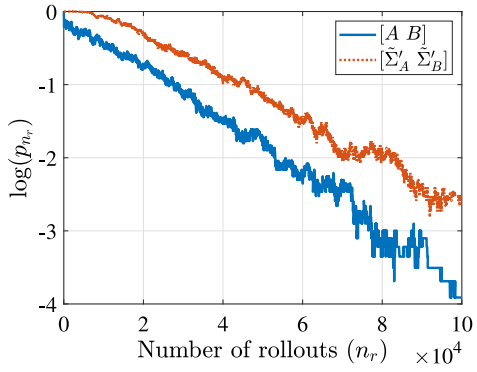

Fig. 2. Finite-sample results of Algorithm 1.

unique, but the following covariance matrix is equivalent to Σ_A,

$$\Sigma_A(\alpha) = \frac{1}{40}\begin{bmatrix} 8 & -2 & 0 & 1+\alpha \\ -2 & 16 & 1-\alpha & 0 \\ 0 & 1-\alpha & 2 & 0 \\ 1+\alpha & 0 & 0 & 8 \end{bmatrix},$$

with $\alpha \in \mathbb{R}$ such that $\Sigma_A(\alpha) \succeq 0$. Fig. 3 illustrates the dynamic (4), starting with the same initial condition $\mu_0 = \mathbf{0}_2$ and $X_0 = \mathbf{0}_4$, and with the noise covariance matrix given by (Σ_A, Σ_B), $(\Sigma_A(1), \Sigma_B)$, and estimates from Algorithm 1, respectively. The parameters of inputs (ν_t and $\bar{U}_t$) are the same as the uniform-input case. Note that $\Sigma_A(-1) = \Sigma_A$, and $\Sigma_A(1) \succ 0$. It can be observed that the dynamics defined by (Σ_A, Σ_B) and $(\Sigma_A(1), \Sigma_B)$ are identical, and the dynamic defined by the estimates from Algorithm 1 is close to the former.

It is assumed that there is no additive noise in System (1), but Algorithm 1 can also be applied to identifying linear systems with both multiplicative and additive noise. If additive noise w_t, independent of the inputs and the multiplicative noise, exists, then write the system as

$$x_{t+1} = (A + \bar{A}_t)x_t + \begin{bmatrix} B + \bar{B}_t & w_t \end{bmatrix}[u_t^T\ 1]^T. \tag{13}$$

In other words, w_t can be considered as a part of multiplicative noise corresponding to a constant input equal to one. Consider the above 2-dimensional system with Gaussian noise $w_t \sim \mathcal{N}(\mathbf{0}_2, \sigma^2 I_2)$ and previously designed Gaussian inputs. Note that in this case $\ell = 6$ is needed because the dimension of inputs increases by one in (13), compared with the original system. Fig. 4 shows the consistency of Algorithm 1 under the presence of additive noise.

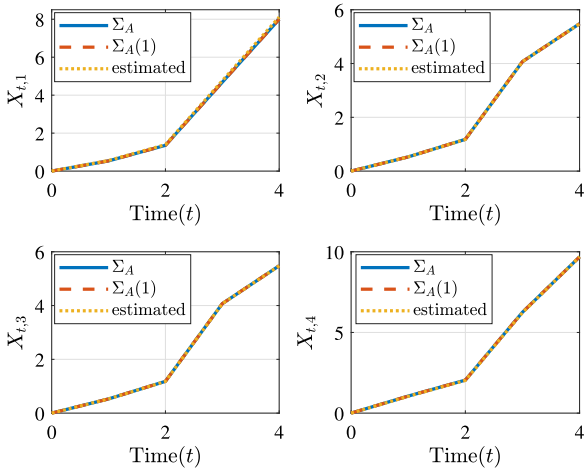

Fig. 3. The second-moment dynamic of system states defined by three noise covariance matrices.

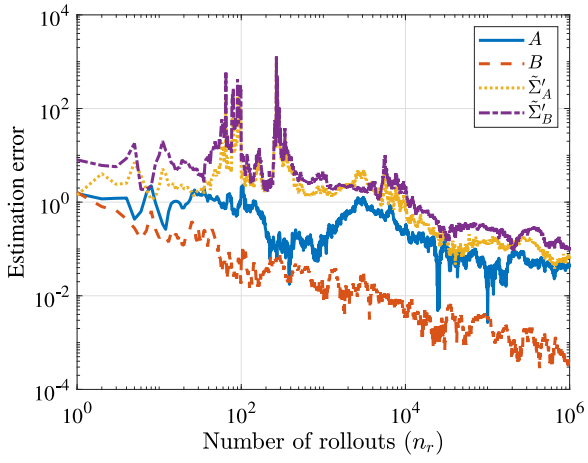

Fig. 4. Consistency of Algorithm 1 under both multiplicative and additive noise.

4.2. Performance comparison

The recursive form of the ordinary least-squares (OLS), namely, the recursive least-squares (RLS), is widely used in identification of dynamic systems (Chen & Guo, 2012; Lai & Wei, 1982). It is possible to apply RLS to identify System (1) if certain conditions hold. For detailed implementation, see Xing et al. (2021). To

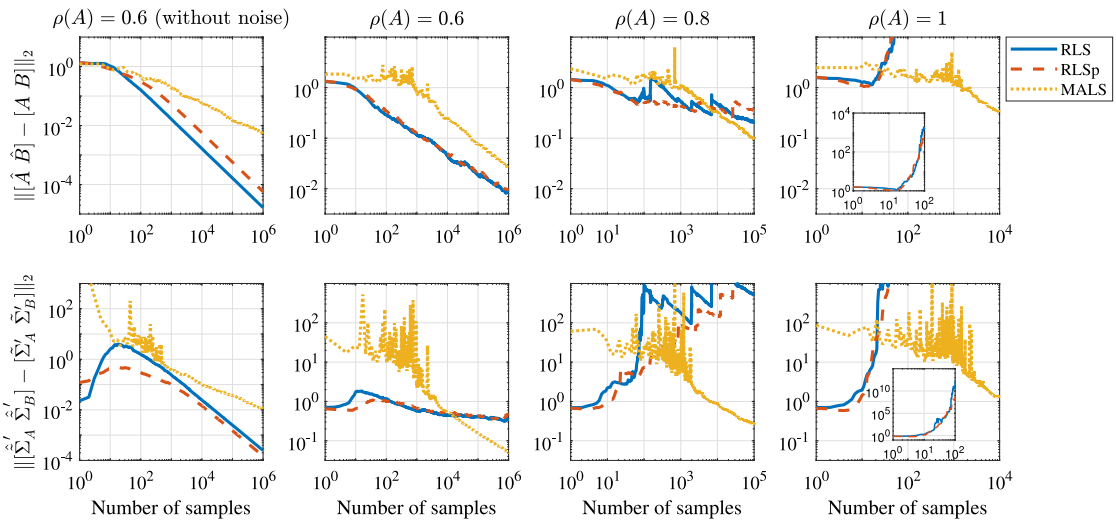

Fig. 5. Performance comparison of RLS, RLSp, and Algorithm 1.

estimate the covariance matrix of the multiplicative noise, Di and Lamperski (2021) apply OLS, which is equivalent to RLS. Note that, when using OLS or RLS, one estimates the second moments of $A+\bar{A}_t$ and $B+\bar{B}_t$, rather than their covariance matrices, which are Σ_A and Σ_B in our context. The estimation of noise covariance is still coupled with the estimation of the nominal system, since $\Sigma'_A = \mathbb{E}\{(A+\bar{A}_t)\otimes(A+\bar{A}_t)\} - A\otimes A$ and $\Sigma'_B = \mathbb{E}\{(B+\bar{B}_t)\otimes(B+\bar{B}_t)\} - B\otimes B$.

To compare the performance of RLS and Algorithm 1, we consider four systems. In the first case, the nominal system matrices are

$$A = \begin{bmatrix} 0.6 & 0.2 \\ 0 & 0.6 \end{bmatrix}, \quad B = \begin{bmatrix} 0.8 \\ 1 \end{bmatrix},$$

and both Σ_A and Σ_B are zero matrices. That is, a linear system without noise and $\rho(A) = 0.6$, where $\rho(A)$ is the spectral radius of A. We use this case to show the consistency of RLS. In the other three cases, the matrix A is set to be

$$\begin{bmatrix} 0.6 & 0.2 \\ 0 & 0.6 \end{bmatrix}, \begin{bmatrix} 0.8 & 0.2 \\ 0 & 0.8 \end{bmatrix}, \text{ and } \begin{bmatrix} 1 & 0.2 \\ 0 & 1 \end{bmatrix},$$

respectively. B is the same as the first case, while Σ_A and Σ_B in Section 4.1 are adopted to be the covariance matrices. The implementation of Algorithm 1 is the same as in Section 4.1. That is, ν_t and $\bar{U}_t$ are randomly generated, and then fixed in all runs of the entire numerical experiment. The input u_t at time $0 \le t \le \ell - 1$ in each rollout is generated from Gaussian distribution $\mathcal{N}(\nu_t, \bar{U}_t)$, and $\ell = 4$. Since RLS is based on single-trajectory data, the length of the trajectory is set to be ℓn_r, so that the number of samples that RLS uses is the same as that of Algorithm 1. RLS with independent standard Gaussian inputs is considered as a baseline. In order to rule out the effect of different input design, we also run RLS with periodic inputs (RLSp) satisfying that, in each period, the inputs are generated in the same way as those in a rollout of Algorithm 1.

For each system, the three algorithms, RLS, RLSp, and Algorithm 1, are run for 50 times, respectively. The mean of estimation error in each case is presented in Fig. 5. It can be observed that RLS and RLSp perform similarly in all cases. When multiplicative noise is absent, they converge slightly faster than Algorithm 1. They are also a little better than Algorithm 1, in the case of $\rho(A) = 0.6$ with noise, for the estimation of $[A\ B]$, indicating OLS could be applied to Algorithm 1 as a way to estimate $[A\ B]$. However, Algorithm 1 surpasses RLS and RLSp when identifying the noise covariance matrix. Moreover, the performance of RLS gets worse as $\rho(A)$ grows. Interestingly, in the case of $\rho(A) = 0.8$, although the nominal system is stable, the second-moment dynamic of system states is not. This instability leads to degraded performance of RLS estimating $[A\ B]$ and divergence of RLS estimating the covariance matrix. In the marginally stable case, namely $\rho(A) = 1$, RLS and RLSp explode in finite time. In contrast, Algorithm 1 behaves almost identically for all cases (the consistency of Algorithm 1 in the marginally stable case is shown in Fig. 1). To sum up, Algorithm 1 can deal with the estimation of noise covariance matrix better and relies less on the stability of both the nominal system and the second-moment dynamic of system states.

5. Conclusion and future work

In this paper an identification algorithm based on multiple-trajectory data was proposed for linear systems with multiplicative noise. With appropriately designed exciting inputs, the proposed algorithm is able to jointly estimate the nominal system and the multiplicative noise covariance. The asymptotic and non-asymptotic performance of the algorithm was analyzed theoretically, and illustrated by numerical experiments. Future work include studying more efficient algorithms that can be used in online settings, optimal and adaptive input design, sparsity-promoting regularization for identification of networked systems, end-to-end finite-sample performance guarantees for identification-based optimal control, and applications to identification of cyber–physical systems with coupling between noise and inputs.

References

Antsaklis, P., & Baillieul, J. (2007). Special issue on technology of networked control systems. *Proceedings of the IEEE*, *95*(1), 5–8.

Boyd, S., El Ghaoui, L., Feron, E., & Balakrishnan, V. (1994). *Linear matrix inequalities in system and control theory*. SIAM.

Breakspear, M. (2017). Dynamic models of large-scale brain activity. *Nature Neuroscience*, *20*(3), 340.

Campi, M. C., & Weyer, E. (2002). Finite sample properties of system identification methods. *IEEE Transactions on Automatic Control*, *47*(8), 1329–1334.

Campi, M. C., & Weyer, E. (2005). Guaranteed non-asymptotic confidence regions in system identification. *Automatica*, *41*(10), 1751–1764.

Chen, H.-F., & Guo, L. (2012). *Identification and stochastic adaptive control*. Springer Science & Business Media.

Coppens, P., & Patrinos, P. (2020). Sample complexity of data-driven stochastic LQR with multiplicative uncertainty. In *IEEE conference on decision and control* (pp. 6210–6215).

Coppens, P., Schuurmans, M., & Patrinos, P. (2020). Data-driven distributionally robust LQR with multiplicative noise. In *Learning for dynamics and control* (pp. 521–530). Proceedings of Machine Learning Research.
Dean, S., Mania, H., Matni, N., Recht, B., & Tu, S. (2019). On the sample complexity of the linear quadratic regulator. *Foundations of Computational Mathematics*, 1–47.
Di, B., & Lamperski, A. (2021). Confidence bounds on identification of linear systems with multiplicative noise. In *American control conference* (pp. 2212–2217).
Du Toit, N. E., & Burdick, J. W. (2011). Robot motion planning in dynamic, uncertain environments. *IEEE Transactions on Robotics*, *28*(1), 101–115.
Duník, J., Straka, O., Kost, O., & Havlík, J. (2017). Noise covariance matrices in state-space models: A survey and comparison of estimation methods, Part I. *International Journal of Adaptive Control and Signal Processing*, *31*(11), 1505–1543.
Gravell, B., Esfahani, P. M., & Summers, T. H. (2021). Learning optimal controllers for linear systems with multiplicative noise via policy gradient. *IEEE Transactions on Automatic Control*, *66*(11), 5283–5298.
Gu, S., Holly, E., Lillicrap, T., & Levine, S. (2017). Deep reinforcement learning for robotic manipulation with asynchronous off-policy updates. In *IEEE international conference on robotics and automation* (pp. 3389–3396).
Guo, Y., & Summers, T. H. (2019). A performance and stability analysis of low-inertia power grids with stochastic system inertia. In *American control conference* (pp. 1965–1970).
Gupta, A. K., & Nagar, D. K. (2018). *Matrix variate distributions*. Chapman and Hall.
Haber, A., & Verhaegen, M. (2014). Subspace identification of large-scale interconnected systems. *IEEE Transactions on Automatic Control*, *59*(10), 2754–2759.
Hespanha, J. P., Naghshtabrizi, P., & Xu, Y. (2007). A survey of recent results in networked control systems. *Proceedings of the IEEE*, *95*(1), 138–162.
Kantas, N., Doucet, A., Singh, S. S., Maciejowski, J., & Chopin, N. (2015). On particle methods for parameter estimation in state-space models. *Statistical Science*, *30*(3), 328–351.
Kitagawa, G. (1998). A self-organizing state-space model. *Journal of the American Statistical Association*, 1203–1215.
Kleinman, D. (1969). Optimal stationary control of linear systems with control-dependent noise. *IEEE Transactions on Automatic Control*, *14*(6), 673–677.
Lai, T. L., & Wei, C. Z. (1982). Least squares estimates in stochastic regression models with applications to identification and control of dynamic systems. *The Annals of Statistics*, *10*(1), 154–166.
Levine, S., Pastor, P., Krizhevsky, A., Ibarz, J., & Quillen, D. (2018). Learning hand-eye coordination for robotic grasping with deep learning and large-scale data collection. *International Journal of Robotics Research*, *37*(4–5), 421–436.
Ljung, L. (1986). *System identification: Theory for the user*. Upper Saddle River, NJ, USA: Prentice-Hall.
Lumley, J. L. (2007). *Stochastic tools in turbulence*. Courier Corporation.
Magnus, J. R., & Neudecker, H. (1980). The elimination matrix: Some lemmas and applications. *SIAM Journal on Algebraic Discrete Methods*, *1*(4), 422–449.
Matni, N., Proutiere, A., Rantzer, A., & Tu, S. (2019). From self-tuning regulators to reinforcement learning and back again. In *IEEE conference on decision and control* (pp. 3724–3740).
Matni, N., & Tu, S. (2019). A tutorial on concentration bounds for system identification. In *IEEE conference on decision and control* (pp. 3741–3749).
Mehra, R. (1970). On the identification of variances and adaptive Kalman filtering. *IEEE Transactions on Automatic Control*, *15*(2), 175–184.
Moghe, R., Zanetti, R., & Akella, M. R. (2019). Adaptive Kalman filter for detectable linear time-invariant systems. *Journal of Guidance, Control, and Dynamics*, *42*(10), 2197–2205.
Schmidt, H., Cho, K.-H., & Jacobsen, E. W. (2005). Identification of small scale biochemical networks based on general type system perturbations. *The FEBS Journal*, *272*(9), 2141–2151.
Schön, T. B., Wills, A., & Ninness, B. (2011). System identification of nonlinear state-space models. *Automatica*, *47*(1), 39–49.
Sun, Y., Oymak, S., & Fazel, M. (2020). Finite sample system identification: Optimal rates and the role of regularization. In *Learning for dynamics and control* (pp. 16–25). Proceedings of Machine Learning Research.
Tropp, J. A. (2015). An introduction to matrix concentration inequalities. *Foundations and Trends in Machine Learning*, *8*(1–2), 1–230.
Tu, S., & Recht, B. (2018). Least-squares temporal difference learning for the linear quadratic regulator. In *International conference on machine learning* (pp. 5005–5014).
Wang, B., Zhang, B., & Su, R. (2020). Optimal tracking cooperative control for cyber-physical systems: Dynamic fault-tolerant control and resilient management. *IEEE Transactions on Industrial Informatics*, *17*(1), 158–167.
Weyer, E., & Campi, M. C. (2002). Non-asymptotic confidence ellipsoids for the least-squares estimate. *Automatica*, *38*(9), 1539–1547.
Wonham, W. M. (1967). Optimal stationary control of a linear system with state-dependent noise. *SIAM Journal on Control*, *5*(3), 486–500.
Xing, Y., Gravell, B., He, X., Johansson, K. H., & Summers, T. (2020). Linear system identification under multiplicative noise from multiple trajectory data. In *American control conference* (pp. 5157–5261).
Xing, Y., Gravell, B., He, X., Johansson, K. H., & Summers, T. (2021). Identification of linear systems with multiplicative noise from multiple trajectory data. arXiv preprint arXiv:2106.16078.
Zheng, Y., & Li, N. (2020). Non-asymptotic identification of linear dynamical systems using multiple trajectories. *IEEE Control Systems Letters*, *5*(5), 1693–1698.

Yu Xing received his B.S. degree in psychology from Peking University in 2014, and his Ph.D. degree in operations research and control theory at Academy of Mathematics and Systems Science, Chinese Academy of Sciences in 2020. Since Sep. 2020 he has been a postdoctoral researcher at the Division of Decision and Control Systems, KTH Royal Institute of Technology, Sweden. His research interests include system identification, social opinion dynamics, network inference, and community detection.

Benjamin Gravell is a Ph.D. student in mechanical engineering with a specialization in control of dynamical systems at The University of Texas at Dallas in Richardson, TX, USA. He earned a B.Sc. degree in mechanical engineering from UT Dallas in 2017. He received the Excellence in Education Doctoral Fellowship awarded by UT Dallas from 2020 to 2022.

His research interests lie at the intersection of data-driven control, estimation, and optimization theory with applications to autonomous robotic systems.

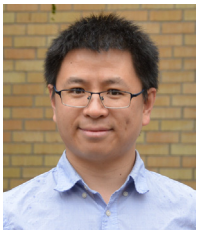

Xingkang He is a postdoctoral research associate in the Department of Electrical Engineering, University of Notre Dame, USA. From Oct. 2018 to Oct. 2021, he was a postdoctoral researcher in the Division of Decision and Control Systems, KTH Royal Institute of Technology, Sweden. He received his Ph.D. degree at the University of Chinese Academy of Sciences in 2018. His research interests include security and privacy of cyber–physical systems, networked control systems, robotics, and machine learning. He received the Best Paper Award in 2018 IEEE Data Driven Control and Learning Systems Conference.

Karl Henrik Johansson is Professor with the School of Electrical Engineering and Computer Science at KTH Royal Institute of Technology in Sweden and Director of Digital Futures. He received M.Sc. degree in Electrical Engineering and Ph.D. in Automatic Control from Lund University. He has held visiting positions at UC Berkeley, Caltech, NTU, HKUST Institute of Advanced Studies, and NTNU. His research interests are in networked control systems and cyber–physical systems with applications in transportation, energy, and automation networks. He is President of the European Control Association and member of the IFAC Council, and has served on the IEEE Control Systems Society Board of Governors and the Swedish Scientific Council for Natural Sciences and Engineering Sciences. He has received several best paper awards and other distinctions from IEEE, IFAC, and ACM. He has been awarded Swedish Research Council Distinguished Professor, Wallenberg Scholar with the Knut and Alice Wallenberg Foundation, Future Research Leader Award from the Swedish Foundation for Strategic Research, the triennial IFAC Young Author Prize, and IEEE Control Systems Society Distinguished Lecturer. He is Fellow of the IEEE and the Royal Swedish Academy of Engineering Sciences.

Tyler H. Summers is an Associate Professor of Mechanical Engineering with an affiliate appointment in Electrical Engineering at the University of Texas at Dallas. Prior to joining UT Dallas, he was an ETH Postdoctoral Fellow at the Automatic Control Laboratory at ETH Zürich from 2011 to 2015. He received a B.S. degree in Mechanical Engineering from Texas Christian University in 2004 and an M.S. and Ph.D. degree in Aerospace Engineering at the University of Texas at Austin in 2007 and 2010, respectively. He was a Fulbright Postgraduate Scholar at the Australian National University in Canberra, Australia in 2007–2008. His research interests are in feedback control, optimization, and learning in complex dynamical networks, with applications to robotics and electric power networks.